JOURNAL OF APPLIED ELECTROCHEMISTRY 17 (1987) 828–840

*Electrochemical surface properties of Co_3O_4 electrodes**

R. BOGGIO, A. CARUGATI†, S. TRASATTI

Department of Physical Chemistry and Electrochemistry, University of Milan, Via Venezian 21, 20133, Milan, Italy

Received 20 August 1986; revised 9 December 1986

The electrochemical behaviour of Co_3O_4 layers deposited by thermal decomposition of $Co(NO_3)_2$ at 200–500° C on titanium supports with and without an interlayer of RuO_2 has been studied by cyclic voltammetry, chronopotentiometry and potential step experiments in alkaline solutions. Such variables as the calcination temperature, the solution pH, the potential sweep rate and the oxide loading have been investigated in detail to determine their influence on voltammetric peaks and voltammetric charge. Insight has been gained into the relevance of the latter to surface area determination and to proton diffusion into the oxide layer. The role of the support–active layer interface and especially that of the RuO_2 interlayer has been scrutinized. The importance of surface studies for the understanding of the electrocatalytic behaviour of Co_3O_4 electrodes has been analysed.

1. Introduction

Co_3O_4 has shown interesting properties as an electrocatalyst for O_2 reduction [1–3] and evolution [1, 4–7], and for Cl_2 production [8–12]. Although the mechanistic details of the above processes have been investigated exhaustively, the basic electrochemical properties of the oxide surface have received little attention. In particular, the degradation of the surface composition under cathodic polarization has been investigated in alkaline solutions [13–16], whereas the anodic behaviour prior to oxygen evolution has been studied only in acid solution where the compound is unstable towards dissolution [17].

The defect structure of Co_3O_4 layers has been investigated by spectroscopic methods in great detail [18–20], while the acid–base response in solution [21] has been studied by measuring the point of zero charge [22]. Co_3O_4 is usually prepared by thermal decomposition of $Co(NO_3)_2$ at temperatures in the range 200 to 500° C [1, 23]. While thermal and X-ray analyses [24, 25] have suggested that the non-stoichiometry of the resulting oxide decreases as the calcination temperature is increased, point of zero charge [22] and chlorine overpotential measurements [10] have indicated that the surface structure is probably independent of the decomposition temperature. The response of the samples to pH variations is typical of oxides and suggests surface enrichment with Co(III) ions, probably as a consequence of the dissolution of lower valency metal ions [21].

The anodic voltammetric curve of Co_3O_4 in alkaline solution shows a characteristic reversible peak just before the evolution of oxygen [1, 7, 15], which has been attributed to the reaction of OH adsorption. However, this peak has not been characterized quantitatively in any detail. The purpose of the present work has been to elucidate the surface behaviour of Co_3O_4 in the region between the open circuit potential and O_2 gas formation for different temperatures of calcination.

* Presented at the 37th Meeting of the International Society of Electrochemistry, Vilnius, USSR, 25–29 August 1986.
† *Present address*: Assoreni, S. Giuliano Milanese (MI), Italy.

0021–891X/87 $03.00 + .12

2. Experimental details

Co_3O_4 electrodes were prepared [25] by thermal decomposition of $Co(NO_3)_2 \cdot 6H_2O$ solutions in isopropanol ($\sim 0.2\,mol\,dm^{-3}$) at the following temperatures: 200, 230, 260, 300, 400 and 500° C. Two sets of electrodes were prepared: in the former group Co_3O_4 was deposited directly onto 10 × 10 × 0.2 mm titanium plates (titanium is the usual support in practical electrodes); in the latter, a thin interlayer of RuO_2 obtained by thermal decomposition of $RuCl_3$ was placed between the support and the active layer. This approach has been prompted by the fact that titanium–Co_3O_4 electrodes show ohmic drop effects related to the oxidation of the underlying metal and that the presence of an interlayer of RuO_2 can alleviate such problems [10]. It is thus necessary to investigate the role of the support–overlayer interface and the possible influence of the nature of the support in view of the possible interferences between the two oxides [26]. In each set, two samples were prepared at each temperature. The electrocatalyst loading was typically 3.6 mg Co_3O_4. Since both faces of the platelets were coated, the effective loading was $1.8\,mg\,cm^{-2}$ of geometric surface, corresponding to a nominal thickness of about 3 μm (nominal density of Co_3O_4 [27], $6.06\,g\,cm^{-3}$). In addition, three (double) samples were prepared at 200° C with catalyst loading of 0.4, 0.9 and $4\,mg\,cm^{-2}$, respectively, to investigate the effect of thickness on the electrochemical response. A total of 30 electrodes were used.

The catalyst was applied layer by layer with a brush to the support which had previously been sandblasted and etched in boiling 20% HCl. The solvent was evaporated at 50–80° C and the deposited nitrate was fired for 10 min at the selected temperature in air. The procedure was repeated until the desired catalyst loading was reached. The samples were then kept for 1 h at the same temperature for final annealing. The samples were mounted into a Teflon electrode holder as described elsewhere [21].

The resistivity of the Co_3O_4 layers was measured by an a.c. technique [28] and was found to be of the order of $10^3\,\Omega$ cm. The additional resistance introduced by the poor conductivity of the oxide was thus of the order of 0.1 Ω in the electrode circuit. This value is small enough not to distort the voltammetric experiments. In fact, no effect was observed on Tafel lines for Cl_2 evolution, while the interference due to the formation of insulating TiO_2 in the absence of the RuO_2 interlayer was quite dramatic [10].

Solutions were prepared volumetrically from Baker KOH (without further purification) and triply distilled water. The three-compartment cell used in this work was described elsewhere [10]. Potentials were measured against a saturated calomel electrode and converted (where necessary) to the RHE or SHE scale using tabulated activity coefficients. Unless otherwise specified, the KOH concentration was $0.9\,mol\,dm^{-3}$ and the temperature 25° C throughout. The solution was deaerated by bubbling purified nitrogen which also provided stirring (which, on the other hand, was observed to have no effects in these experiments).

This study was carried out by means of three different techniques: cyclic voltammetry, chronopotentiometry and potential step. The equipment consisted of a potentiostat–galvanostat coupled with a function generator and an X–Y recorder (all AMEL).

Voltammetric curves were usually recorded after keeping the electrode at the open circuit potential for 5 min and cycling for an additional 5 min. Unless otherwise specified, the sweep rate was $10\,mV\,s^{-1}$. The potential range scanned was usually 600 mV into the anodic region.

In the other experiments the electrode was conditioned at the initial potential for 5 min and then the current or potential step was applied. In all cases, the electrodes were first reconditioned at a potential equal to that of the open circuit before being extracted from the solution.

3. Results and discussion

3.1. *Open circuit potential*

Fig. 1 shows the effect of the temperature of preparation on the open circuit potential. It has been shown in a previous paper [21] that the value of this potential can be understood in terms of the surface equilibrium reaction,

$$Co_3O_4 + 2H_2O \rightleftharpoons 3CoOOH + H^+ + e \quad (1)$$

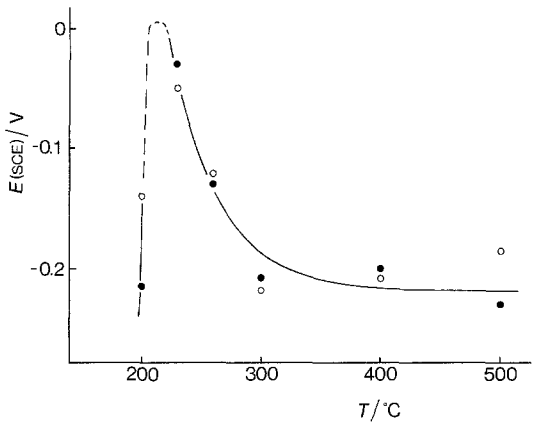

Fig. 1. Dependence of the open circuit potential of titanium–Co_3O_4 electrodes with (●) and without (○) a RuO_2 interlayer on the calcination temperature. KOH solution, 4.5 mol dm^{-3}.

the observed value depending specifically on the ratio of the two oxide forms. Although the measured potentials have no strict thermodynamic significance, a steep rise is observed as the temperature of calcination is lowered, with a break at about 210° C. Since Co_3O_4 is known [25] to become increasingly non-stoichiometric by metal vacancies as the preparation temperature is decreased, the data in Fig. 1 can be explained in terms of an increasing Co(III)/Co(II) ratio under these conditions.

No systematic variation of the open circuit potential with the preparation procedure was observed in the previous work [21]. This may be due to two reasons: (a) samples were not prepared at 230 and 260° C where the maximum effect can be seen in Fig. 1; (b) the details of the preparation were different. Also, in the case of pzc measurements [22] no effect of the calcination temperature was observed, but in that case powders were used which were subjected to 12 h decomposition. However, the same electrodes were used for chlorine evolution in other work and again no effect of the temperature of preparation was observed (besides the surface area change) [10]. This may be due to the fact that chlorine evolution is a 'non-demanding' reaction. Alternatively, the anodic polarization may induce a lattice ordering [16] which smooths down the differences at the open-circuit potential.

The break at about 210° C in Fig. 1 probably indicates a phase modification. Although at this temperature only Co_3O_4 is thermodynamically present [25], its formation may require a longer time than that allowed for the decomposition in this work. Therefore, the surface composition may be somewhat more reduced at 200° C.

In general, no systematic effect of the presence of the RuO_2 interlayer is observed in Fig. 1. However, at 200° C the potential is much more negative for the sample with RuO_2. Since the catalyst is very finely dispersed at this temperature, the solution may reach the interlayer which possesses an appreciably more negative open circuit potential [29].

The same pattern is maintained as the KOH concentration is varied from 4.5 to 0.09 mol dm^{-3}.

3.2. *Voltammetric curve*

Fig. 2a shows the characteristic shape of the voltammetric curve between the open circuit potential and oxygen evolution. There is a single anodic peak at 390 mV (SCE), ~ 1.45 V (RHE). There is a corresponding cathodic peak but it is lower and broader. Varying the potential sweep rate reveals a shoulder in the cathodic peak (Fig. 2b). This probably indicates a splitting of the cathodic process. No significant difference in the general shape of the voltammetric curve can be observed between samples with and without the RuO_2 interlayer.

The value of the potential suggests that the peak is associated with the complete oxidation of the surface of Co_3O_4 to Co(IV) according to the reaction

$$CoOOH \rightleftharpoons CoO_2 + H^+ + e \quad (2)$$

which, according to Pourbaix's diagram [30], should take place at 1.48 V (RHE). A peak at the same potential has also been observed by Burke *et al.* [31, 32] on cobalt under potential cycling conditions. These authors have assigned the peak to the same reaction. The present interpretation differs from that given by Tarasevich and co-workers [1, 7, 15], according to whom the peak is related to OH adsorption through $2OH \rightleftarrows H_2O_2 + 2e$. The explanation was based on an observed peak potential shift of 0.14 V per pH unit which has not been confirmed in this work.

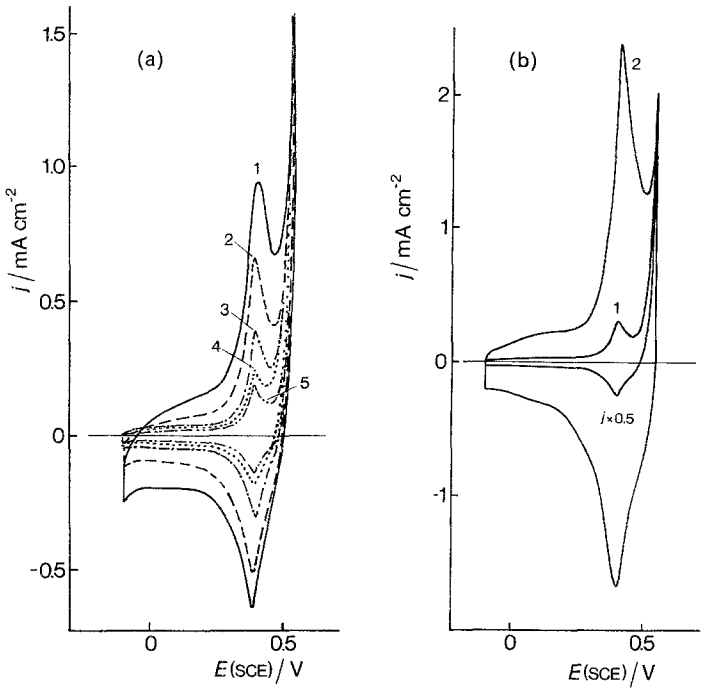

Fig. 2. (a) Voltammetric curves at $10\,mV\,s^{-1}$ in $0.9\,mol\,dm^{-3}$ KOH solution of titanium–Co_3O_4 electrodes with a RuO_2 interlayer prepared at various temperatures: (1) 230, (2) 260; (3) 300, (4) 400, (5) 500° C. (b) Effect of the potential sweep rate on the voltammetric curve in $0.9\,mol\,dm^{-3}$ KOH solution of a titanium–Co_3O_4 electrode prepared at 400° C with a RuO_2 interlayer. (1) $10\,mV\,s^{-1}$; (2) $200\,mV\,s^{-1}$.

If the peak is due to Reaction 2 and the open-circuit potential to Reaction 1, the residual Co(II) ions are oxidized to Co(III) somewhere within this potential region. If the cathodic limit of the voltammetric curve is extended, other peaks appear clearly. This is shown in Fig. 3 where the cathodic shoulder is also evident. The main peak is seen not to be affected by the cathodic limit up to about −0.5 V (SCE), ~0.55 V (RHE), but two clear peaks can be seen at about 0.09 and −0.2 V (SCE), ~1.15 V and 0.85 V (RHE) respectively. These peaks are much lower and the ratio of their area to that of the main peak is about 1 to 3. Therefore, the peak at 1.15 V probably corresponds to the reverse of Reaction 1. The composition corresponding to Co_3O_4 is thus reached at about 1 V, close to the open-circuit potential.

The more cathodic peak corresponds to a more reduced composition than Co_3O_4 and may be associated with the reaction [30]:

$$Co_3O_4 + 2H_2O + 2H^+ + 2e \rightleftharpoons 3Co(OH)_2 \quad (3)$$

However, the charge associated with this peak should be twice that associated with the next anodic peak. It may be that reduction takes place in steps. This is corroborated by the observation that if the cathodic limit is extended past ~ −0.50 V (SCE), the curve becomes less symmetric and ultimately a new peak appears at about −0.56 V (SCE), ~0.50 V (RHE). It is

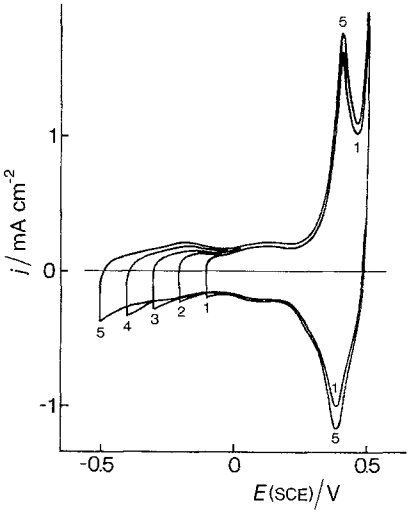

Fig. 3. Effect of the cathodic potential limit on the voltammetric curve in $0.9\,mol\,dm^{-3}$ KOH solution at $20\,mV\,s^{-1}$ of a titanium–Co_3O_4 electrode prepared at 400° C. Potential range: (1) 0.6, (2) 0.7, (3) 0.8, (4) 0.9, (5) 1.0 V. Initial potential, 0.50 V (SCE) ≃ 1.55 V (RHE).

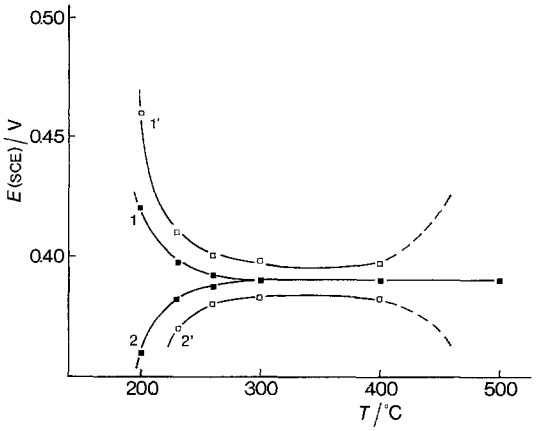

Fig. 4. Potential of the anodic (1,1′) and cathodic (2,2′) main peaks as a function of the calcination temperature for titanium–Co_3O_4 electrodes with (1,2) and without (1′,2′) a RuO_2 interlayer.

possible that the reduction of Co_3O_4 proceeds first to a less hydrous and then to a more hydrous reduced species [31]. It is intriguing that the formation of the most cathodic peak does not affect the shape and the position of the main peak, but the evolution of oxygen is progressively enhanced.

It has been observed that the height and the position of the main peak is no longer affected as the anodic potential limit is extended into the oxygen evolution region. This clearly indicates that oxygen evolution occurs on an oxide surface fully oxidized to Co(IV) and that no further surface oxidation takes place during the oxygen formation.

3.2.1. Effect of the calcination temperature. Fig. 2a shows that the position of the main peak is little influenced by the calcination temperature, although a small systematic shift is detectable (see later). The main varying feature is that the lower the calcination temperature the higher the asymmetry of the curve close to the open circuit potential, i.e. the current is markedly cathodic in this potential region. This indicates that the oxidized surface is not stabilized. In this respect there is a systematic variation of the shape of the curve with temperature.

Fig. 4 shows the dependence of the peak potentials on the temperature of calcination. Electrodes without RuO_2 show a systematically more anodic peak. At 500° C without RuO_2 the curve is completely deformed and none of the typical features can be recognized. This is associated with the formation of an insulating TiO_2 film whose presence can be recognized in kinetic experiments [10]. The deviation of the peak from the typical value of 0.39 V (SCE) for electrodes without RuO_2 can be understood along the same lines [10].

As the calcination temperature is lowered the anodic peak potential becomes more positive. At the same time the cathodic peak shifts so that the pairs move further apart. Although this phenomenon might indicate an increasingly irreversible process because of a change in the catalyst surface composition, this interpretation is not substantiated by other observations (see later). Moreover, the peaks move further apart upon prolonged anodization [10] which should, in fact, result in a more stoichiometric and more stable oxide [15]. Therefore, the low temperature deviation of the peak potential can still be understood in terms of TiO_2 film formation. Since the catalyst is very fine and disperse it is likely to be poorly protective and the support can presumably be reached by the solution through pores.

3.2.2. Effect of potential sweep rate. Fig. 5 shows the effect of sweep rate on the position of the anodic peak. A similar pattern is also observed for the cathodic peak. There is always a drift towards more positive values as the sweep rate increases (and the reverse occurs with the cathodic peak). The shift is minimum (~ 20 mV) for the samples prepared at 300–500° C. The effect is more appreciable for the electrodes without RuO_2. This fact indicates that the effect of the sweep rate is very likely to be associated with uncompensated ohmic drop effects which are higher in the absence of the RuO_2 interlayer because the formation of the insulating TiO_2 film is not prevented. Similar effects have recently been determined through simulation [33].

Although the moving apart of the two main peaks as the sweep rate is increased might also be due to uncompensated ohmic drops in the solution only, it has been verified that the observed phenomenon is not affected by varying the position of the electrode with respect to the capillary of the reference electrode compartment. In fact,

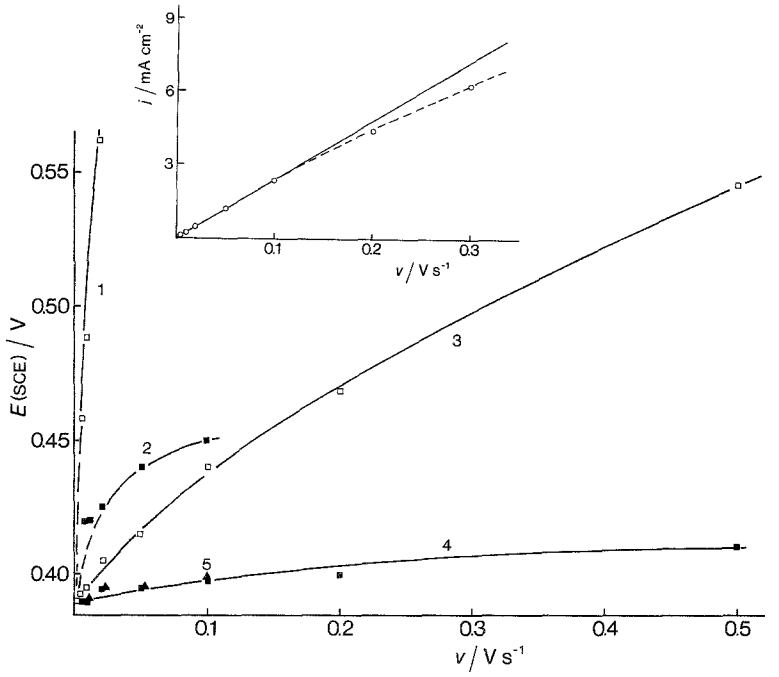

Fig. 5. Potential of the main anodic peak as a function of the potential sweep rate for titanium–Co_3O_4 electrodes with (■,▲) and without (□) a RuO_2 interlayer prepared at various temperatures: (1,2) 200, (3,4) 400, (5) 500° C. Inset: current at the main anodic peak as a function of potential sweep rate for a titanium–Co_3O_4 electrode prepared at 400° C.

the shift of E_p has been observed to be proportional to the deviation of the peak from 390 mV in Fig. 4. It is to be noted that this deviation is larger for the sample prepared at 200° C with RuO_2 than for the sample prepared at 400° C without RuO_2. Nevertheless the sample prepared at 200° C appears to shift less in Fig. 5. It might be that part of the deviation is due to some modification in the surface composition. However, the response of the underlying RuO_2 should also be taken into account for this specific sample.

The dependence of the peak current on the potential sweep rate has also been determined. The slope of the log–log plot has been observed to be very close to one, the closer the higher the calcination temperature (see Fig. 5, inset). This confirms that the reaction can be considered as a highly reversible surface redox process. The deviations from the unit slope are probably associated with *IR* drops. Also, in the case of the samples prepared at 200° C, with and without RuO_2, the surface process is substantially reversible.

3.2.3. Effect of pH. The pH does not affect the peak current but shifts the peak potential. Fig. 6 shows the pH dependence of the peak potential. While the peak position depends on the calcination temperature (cf. Fig. 4), the slope of the pH dependence is substantially independent of it. No systematic dependence on whether RuO_2 is present or not can be recognized, but the

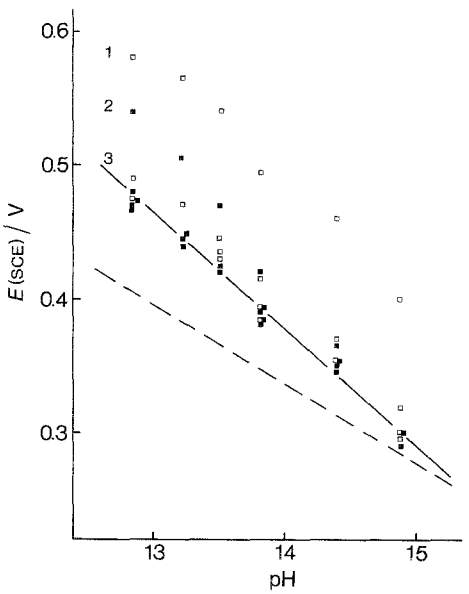

Fig. 6. Potential of the main anodic peak as a function of solution pH (KOH) for titanium–Co_3O_4 electrodes with (●) and without (○) a RuO_2 interlayer prepared at various temperatures: (1,2) 200, (3) ⩾230° C.

sample at 200° C with RuO_2 exhibits a higher slope, which may again be related to the direct influence of the interlayer.

Fig. 6 shows that the slope is higher than that expected from Reaction 1. It is about 88 mV per pH unit, much lower than the slope of 140 mV claimed by Tarasevich and Efremov [1, 7]. Similar slopes are not uncommon with oxides from voltammetric measurements [34]. They have been interpreted in terms of formation of surface oxyanions. However, the value of the slope calls for a fractional charge on the surface complex. It is probable that these slopes are determined by other factors. In fact, open-circuit (equilibrium) potentials usually show a Nernstian behaviour [21, 29, 35]. Surface processes involve adsorption of intermediates and it is known that pre-waves or post-waves can appear, depending on whether the product or the reactant is adsorbed. The position of the wave depends on the surface-intermediate bond strength. It is thus possible that the adsorption of intermediate (OH) on the surface under oxidation is energetically affected by its state of charge which is pH-dependent for oxides [36]. This may be responsible for the observed deviation from the classic Nernst response. A similar reason has been proposed [37] to explain the observed fractional reaction order for oxygen evolution on oxides. At any rate, in the case of Co_3O_4, the peak potential (at 10 m V s^{-1}) shifts faster than the start of oxygen evolution; thus, E_p comes closer and closer to E_{O_2} as the pH is decreased. Therefore, oxygen evolution very likely takes place in acid solution on a more reduced surface with a strongly positive charge (the pzc of Co_3O_4 is 7.5 [22]).

3.3. *Voltammetric charge*

The voltammetric charge was determined by integration of the current–potential curves in Fig. 2a up to the potential of incipient oxygen evolution. This charge, henceforth denoted q^*, is associated with Reactions 1 and 2. The anodic and cathodic charges have been found to be equal, which substantiates the qualitative idea, based on the data in Fig. 2b, that the cathodic main peak is in fact a doublet with a ratio of approximately 1 to 2.

The value of the voltammetric charge shows good reproducibility. If extensive anodic processes take place, q^* has been shown [10] to drift slowly with the electrode use. This aspect will not be considered further here. Voltammetric charges have already been used to characterize the surface structure and properties of such oxide electrodes as IrO_2 [35], RuO_2 [38] and $NiCo_2O_4$ [39].

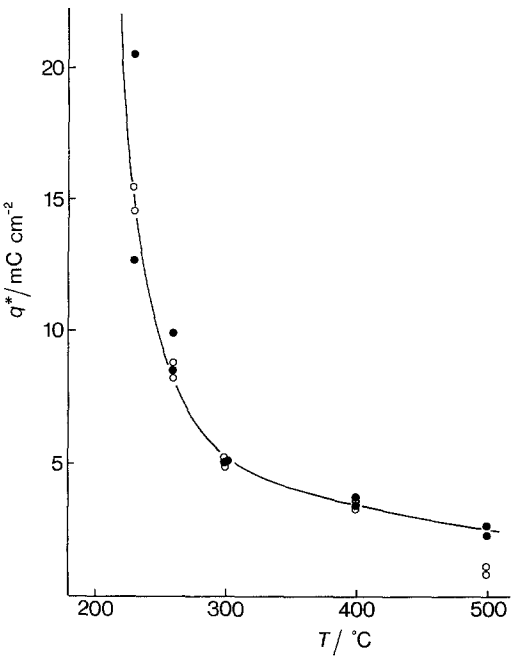

Fig. 7. Charge obtained by integration of the voltammetric curves in Fig. 2 as a function of the calcination temperature for titanium–Co_3O_4 electrodes with (●) and without (○) a RuO_2 interlayer.

3.3.1. Effect of the calcination temperature. Fig. 7 shows the dependence of q^* on the decomposition temperature. Values of q^* are seen to decrease dramatically as the calcination temperature is raised. No substantial difference is observed at $T \geqslant 260°$ C between samples with RuO_2 and samples without the interlayer. Therefore, the surface characteristics do not depend on the structure and nature of the underlying surface. At $T < 260°$ C, points are more scattered, thus confirming that this temperature range is a very crucial one for the decomposition process (cf. Fig. 1). Again, no systematic effect of the nature of the support can be recognized. The discrepancies at 500° C, between electrodes

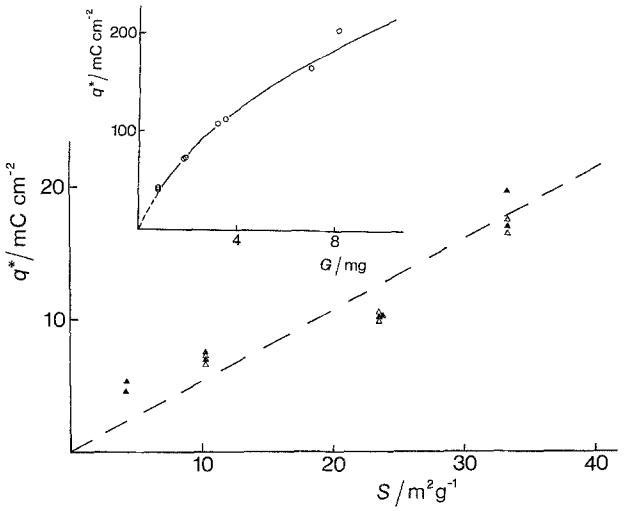

Fig. 8. Plot of the voltammetric charge of titanium–Co_3O_4 electrodes (from Fig. 7) versus the BET surface area of powder samples prepared at the same temperature (from [25]). Inset: voltammetric charge as a function of oxide loading for titanium–Co_3O_4 electrodes prepared at 200° C.

with and without RuO_2, result from the deformation of the voltammetric curve in the absence of the interlayer due to ohmic drop effects.

The decrease of q^* with increasing temperature is attributable to syntering and crystal growth as X-ray analysis has shown [25]. Therefore, the drop in q^* is evidence of a decrease in the surface area exposed to the solution. Since the charge associated with a monolayer of monovalent substance is of the order of 0.1 mC cm^{-2} [40], the roughness factor of Co_3O_4 appears to vary approximately from 10 at 500° C up to 1000 at 200° C. (This refers to a nominal thickness of 3 μm.)

In principle, q^* may be associated not only with surface transformations but also with bulk modifications. There is no unambiguous way of determining the real surface area of planar solid electrodes. Since the structure of the catalyst is that of a pressed powder, its surface is thought to be proportional to that determined by gas adsorption (BET method) using powders. Fig. 8 shows a correlation between BET surface area [25] and q^* values on samples prepared at the same temperature but of different shape, and also shows that the points, though scattered, tend to group around a straight line which has a unit slope on a log–log plot. This indicates that q^* changes proportionally to the real surface area. This is in line with the fact that the sharpness of the main peak is indicative of a purely surface process.

3.3.2. Effect of oxide loading. It has been found that q^* increases with increasing oxide loading. The dependence is, however, non-linear as shown in the inset of Fig. 8. This indicates that some of the crystallites remain progressively excluded from the contact with the solution as the layer grows. In general, linear dependence on oxide loading has been observed with RuO_2 [40] and IrO_2 [35] but only below a critical thickness. The data for Co_3O_4 in the inset of Fig. 8 refer to samples without RuO_2 which could interfere because this oxide is known to be subjected to substantial proton penetration [41].

3.3.3. Effect of pH. The value of q^* has been observed to stay approximately constant as the pH is changed for samples prepared at temperatures $\geqslant 300°$ C, while some variation is apparent for lower calcination temperatures. However, since the main peak moves faster than oxygen evolution as the pH is decreased, it is difficult to integrate the curve over a perfectly equivalent potential range, especially for the samples which exhibit a distortion of the voltammetric curve. On the other hand, the variation has not been found to be higher than $\sim 10\%$. Therefore, the results indicate that the surface charge does not depend substantially on pH.

3.3.4. Effect of potential sweep rate. As is shown in Fig. 9, q^* decreases as the sweep rate is increased. The rate of decrease is larger for

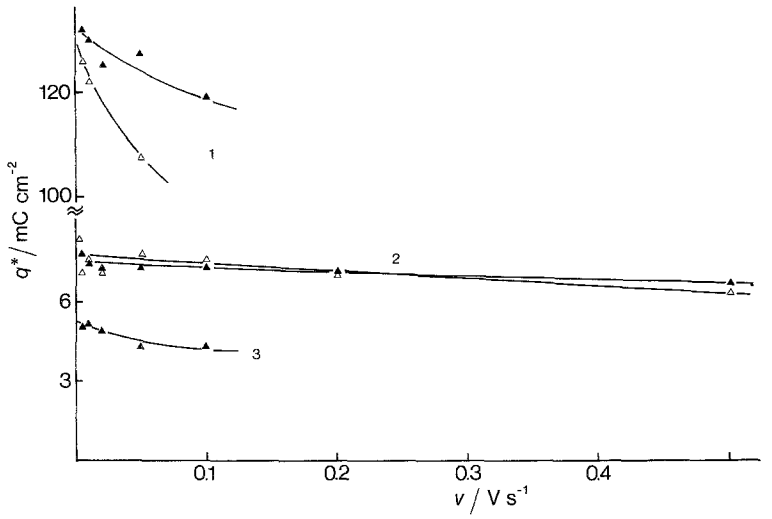

Fig. 9. Voltammetric charge as a function of potential sweep rate for titanium–Co_3O_4 electrodes with (▲) and without (△) a RuO_2 interlayer, prepared at various temperatures: (1) 200, (2) 400, (3) 500° C.

electrodes without the RuO_2 interlayer. This indicates that at least part of the variation of q^* is simply associated with a distortion of the voltammetric curve and no definite physical meaning can be attached to it. However, the decrease of q^* for electrodes with a RuO_2 interlayer is real and is presumably associated with a slow step in the electrode reaction. Since this is essentially a proton exchange reaction (cf. Reactions 2 and 3) the experimental observations indicate that part of the surface of the electrode is of difficult accessibility to protons, whose supply to these confined regions decreases as the sweep rate is increased. The 'internal' surface may be the inner wall of pores, the grain boundaries and the intercrystallite regions. The slow step is therefore thought to be the surface diffusion of protons (or OH^-).

3.4. *Surface area estimation*

Voltammetric curves can, in principle, be used to measure surface areas. This implies that the capacity of the given interface must be known. This method has been proposed [42, 43] as being suitable in the case of high surface area oxide electrodes. The purpose of this section is to show that such a proposal cannot have any general validity.

Voltammetric curves were recorded at different potential sweep rates over a potential range of 50 mV. There is no so-called double layer region with Co_3O_4 (cf. Fig. 2). Therefore, experiments were performed in three different potential regions: 0–0.05 V, 0.1–0.15 V and 0.30–0.35 V (SCE) (regions A, B, C, respectively).

Voltammetric curves at different sweep rates have shown that the shape remains the same as v increases, but it is quite different in regions A and C. The dependence of the current (measured at a potential in the middle of the region) on the sweep rate has been found to be non-linear, as expected (cf. Fig. 5, inset), and the current is of course different in the different potential regions. Since non-linearity is thought to be due to 'inner surface area' exclusion, the slope of the dependence, which corresponds to a differential capacitance,

$$\mathrm{d}j/\mathrm{d}v = \mathrm{d}(q/t)/\mathrm{d}(E/t) = \mathrm{d}q/\mathrm{d}E = C \quad (4)$$

has been measured at $v \to 0$.

In region A, outside the peaks, the capacitance has been found to be 2.4 mF cm^{-2}. If this figure is divided by 80 μF cm^{-2}, a 'possible' value of C for the oxide–solution interface [22, 35], the resulting value for the real surface area is 30 cm^2. The roughness factor is thus 30. The total charge of this electrode is 7.1 mC cm^{-2} geometric surface (cf. Fig. 7). Therefore, the charge exchanged per unit real surface area is estimated to be $\sim 120\,\mu$C cm^{-2}. This is a reasonable figure for a surface exchanging about 1.3 electrons per surface metal atom in the potential range explored.

If the calculation is repeated for the data in region B, the capacitance is 2.8 mF cm^{-2}, giving a real surface area of 35 cm^2. In region C the

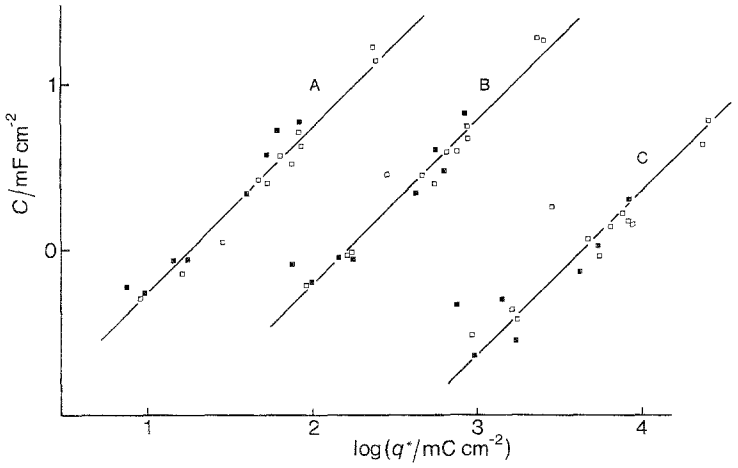

Fig. 10. Apparent capacitance of titanium–Co_3O_4 electrodes with (■) and without (□) a RuO_2 interlayer as a function of the total voltammetric charge. A, B and C refer to three different potential ranges (see text). ——, Straight lines of unit slope. B has been shifted horizontally; C has been shifted both horizontally and vertically.

capacitance is 11.5 mF cm^{-2} and the estimated real surface area is about 144 cm^2. The charge exchanged per unit real surface area now becomes 25 μC cm^{-2}. The current read in region C undoubtedly contains a faradaic component, therefore the last figure is the least reliable. Also in regions A and B, however, the current does not involve simply double-layer charging, although the dependence of the open circuit potential of oxides is interpreted in terms of proton exchange in potentiometric titration and in terms of electron exchange in electrode equilibria. In any case, the estimated surface area, based on capacitance measurements, is not unambiguous.

Fig. 10 shows a plot of the apparent capacitance of the interface as a function of the total voltammetric charge. In regions A, B and C the two quantities are linearly related and the slope of the log–log plot is strictly unity. This indicates that over all the explored potential range the whole surface is involved in charge exchange phenomena. There is, therefore, no difference in using either quantities C and q^* as a *relative* measure of surface area, but the use of a specific value of capacitance to derive the true surface area must clearly be ruled out.

3.5. *Current step experiments*

With the purpose of elucidating the possible proton surface diffusion phenomena pointed out above, current and potential step experiments were performed. In current step experiments the electrode was kept at 0 V for 5 min, then the current was stepped anodically and the charge necessary to drive the potential up to 0.3 V (SCE) was obtained from the chronopotentiometric curve.

Fig. 11 shows that the measured charge decreases noticeably with increasing current density. The rate of decrease depends on the calcination temperature. If the data are replotted against $t^{1/2}$, where t is the transition time from 0 to 0.3 V, the plot is linear at longer times and shows a break at shorter times (Fig. 11, inset). A similar dependence has been observed with RuO_2 electrodes [44] and indicates that a diffusion phenomenon limits the surface charge exchange. The slope of the linear plot is proportional to the diffusion rate. If the diffusion coefficient of the species is reasonably constant and the thickness of the layer is the same, the diffusion rate can only depend on the proton concentration gradient, which depends on the proton uptake capacity of the surface, namely on its extent.

The inset in Fig. 11 shows that q^* is larger at shorter times for cathodic current steps, while the slope is higher for anodic current steps. The reason for this is not clear quantitatively, but it is probably related to the presence of the RuO_2 interlayer. In fact, in the absence of the interlayer, the anodic and cathodic slopes are very close. This is illustrated in Fig. 12, where the surface diffusion rate is plotted against q^*, measuring the extension of the electrochemically active surface. While a broad trend for the rate

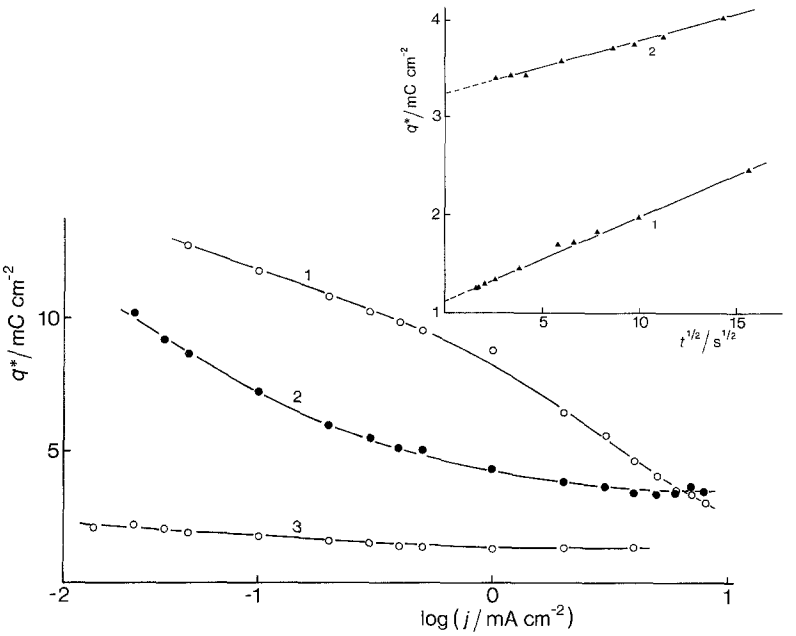

Fig. 11. Dependence of charge on current in chronopotentiometric experiments with titanium–Co_3O_4 electrodes with (●) and without (○) a RuO_2 layer, prepared at various temperatures: (1) 230, (2) 260, (3) 300° C. Potential interval, 0 to 0.3 V (SCE). Inset: plot of charge versus square root of transition time in chronopotentiometric experiments with a titanium–Co_3O_4 electrode prepared at 300° C with a RuO_2 interlayer. (1) Anodic current pulse; (2) cathodic current pulse.

to increase with q^* can be recognized, a closer inspection shows that the points probably gather into two groups: anodic current steps in one group and all the others in another group with lower rates. It seems that the higher diffusion rate for group A might be related to the buffering action of the RuO_2 interlayer which takes up protons during the cathodic charging pretreatment. This explanation is tentative, but the effect of the presence of the RuO_2 interlayer is recognizable.

3.6. *Potential step experiments*

Potential step experiments are more suited to the quantitative investigation of diffusion processes in the solid state, since the rate of the interfacial reaction is not driven from the exterior. Anodic and cathodic potential steps were applied to the electrode kept at the initial potential for 5 min. Anodic steps of 0.15, 0.30 and 0.45 V started from 0 V. Cathodic steps of the same amplitude started from 0.45 V (SCE) just at the onset of oxygen evolution.

Current–time curves were integrated to obtain charge–time curves. If q^* is plotted as a function of $t^{1/2}$, the dependence is strictly linear at times longer than about 4 s. The slope of the straight line, if plotted against the calcination temperature, exhibits a variation parallel to that of q^*. This is well illustrated in Fig. 13 where the diffusion rate is plotted against the voltammetric charge. The rate is seen to increase almost linearly with the extent of the surface, but the rate of increase is higher for the samples with RuO_2. This is true also for cathodic steps. There are divergencies between anodic and cathodic

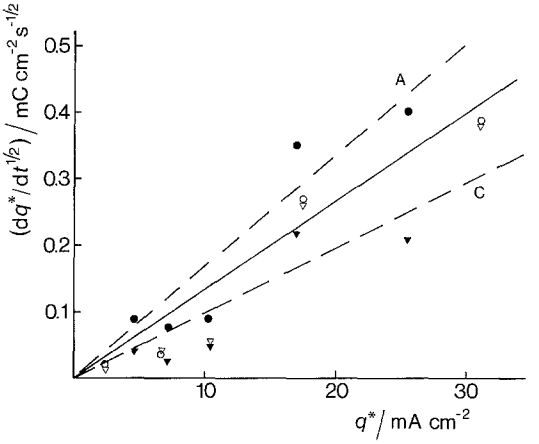

Fig. 12. Slope of the straight lines, such as those in the inset of Fig.11 plotted vs the total voltammetric charge for titanium–Co_3O_4 with (●,▼) and without (○,▽) a RuO_2 interlayer. (——) Broad general trend. (A) Trend for anodic (●,○) experiments; (C) Trend for cathodic (▼,▽) experiments.

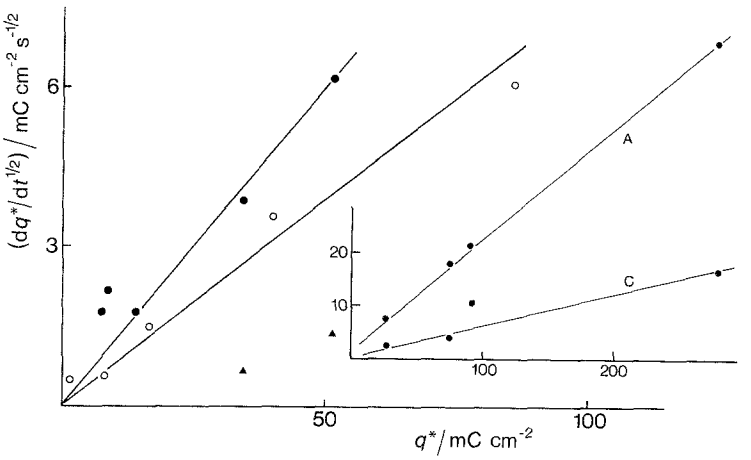

Fig. 13. Plot of the slope of q^*–$t^{1/2}$ plots in potential step experiments versus the total voltammetric charge for titanium–Co_3O_4 electrodes with (●) and without (○) a RuO_2 interlayer. Anodic potential step 0 → 0.45 V (SCE). (▲) Experiments at pH = 8.4. Inset: the same plot for the samples prepared at 200° C with different oxide loading. (A) Anodic and (C) cathodic potential steps between 0 and 0.45 V (SCE) are distinguished.

potential steps; this is dramatically evident for samples (without RuO_2) with different catalyst loading, as Fig. 13 (inset) shows. A summary of the data is given in Fig. 14 by plotting the slope of the q^*–$t^{1/2}$ straight lines for cathodic steps against those for the corresponding anodic step. As Fig. 14 shows, the two sets of data are linearly related. The slope of the relationship is unity for electrodes with RuO_2, but the lines do not go through the origin. The higher anodic slope may be related to the buffering action of RuO_2 which acts as a reservoir of protons.

An explanation for the higher anodic slopes in the case of electrodes without RuO_2 is more difficult. The deviation becomes detectable at temperatures $\leqslant 300°$ C, where the effect of the support becomes important. There are two possibilities: (a) the potential steps are distorted by the ohmic drop due to an interlayer of insulating TiO_2 (but why the steps are asymmetric is difficult to envisage quantitatively); (b) the interlayer of TiO_2 grows during the anodic step, but it does not contribute to the current during the cathodic step. The latter hypothesis seems probable in the light of previous kinetic studies [10]. The idea that the current in potential step experiments is limited by the difficult accessibility of internal surface regions is substantiated by some experiments at about pH 8. Fig. 13 shows that the rate of charge exchange is much lower, which is probably related to the difficulty of supply of protonic species to the inner surface during charging.

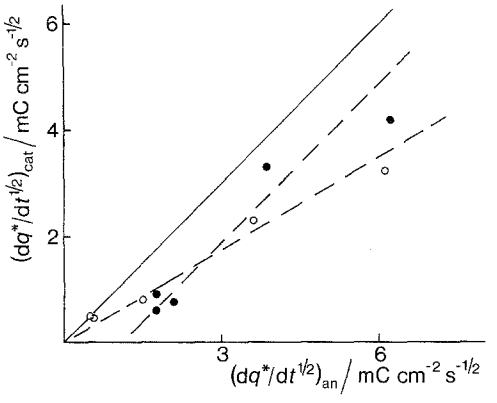

Fig. 14. Graphical comparison of the slopes of q^* versus $t^{1/2}$ plots for anodic and cathodic potential steps. ——, Linear correlation of unit slope. Linear correlations for titanium–Co_3O_4 electrodes with (○) and without (●) a RuO_2 interlayer are indicated.

4. Conclusions

1. Co_3O_4 is reversibly oxidized and reduced prior to oxygen evolution through a reaction involving proton exchange with the solution.

2. Oxygen evolution takes place on a surface where all cobalt ions are in the +4 oxidation state. No further oxidation takes place at higher potentials.

3. The charge associated with the main surface reaction is proportional to the working surface. However, part of the latter is of difficult accessibility and is probably associated with grain boundaries, intercrystallite regions and pores.

4. Co_3O_4 does not protect the underlying

metal (titanium) totally. The lower the calcination temperature the more appreciable the phenomena attributable to the support.

5. RuO_2 prevents the formation of an insulating layer of TiO_2, but its influence on the behaviour of the Co_3O_4 overlayer becomes evident in proton diffusion experiments while the chemical features of the external surface are not affected.

6. The critical temperature for Co_3O_4 formation on a support with short firing times (10 min) is 230° C.

7. The quantitative estimation of the real surface area of Co_3O_4 electrodes from voltammetric charging processes is an ambiguous procedure which can only give the order of magnitude provided the choice of the potential range to explore is based on objective criteria.

Acknowledgement

Financial support to this work by the Italian National Research Council (CNR), Rome, is gratefully acknowledged.

References

[1] M. R. Tarasevich and B. N. Efremov, in 'Electrodes of Conductive Metallic Oxides', Part A (edited by S. Trasatti), Elsevier, Amsterdam (1980) p. 221.
[2] V. S. Bagotsky, N. A. Shumilova and E. I. Khrushcheva, *Electrochim. Acta* **21** (1976) 916.
[3] A. M. Trunov and V. A. Presnov, *Elektrokhimiya* **11** (1975) 77.
[4] C. Iwakura, A. Honji and H. Tamura, *Electrochim. Acta* **26** (1981) 1319.
[5] A. C. C. Tseung and S. Jasem, *ibid.* **22** (1977) 31.
[6] S. Trasatti, *ibid.* **29** (1984) 1503.
[7] B. N. Efremov and M. R. Tarasevich, *Elektrokhimiya* **17** (1981) 1672.
[8] M. B. Konovalov, V. I. Bystrov and V. L. Kubasov, *ibid.* **12** (1976) 1266.
[9] D. L. Caldwell and M. J. Hazelrigg, in 'Modern Chlor-alkali Technology' (edited by M. O. Coulter), Ellis Horwood, Chichester (1980) p. 121,
[10] R. Boggio, A. Carugati, G. Lodi and S. Trasatti, *J. Appl. Electrochem.* **15** (1985) 335.
[11] R. A. Agapova and G. N. Kokhanov, *Elektrokhimiya* **12** (1976) 1649.
[12] V. V. Shalaginov, D. M. Shub, N. V. Kozlova and V. N. Lomova, *ibid.* **19** (1983) 537.
[13] B. N. Efremov, M. R. Tarasevich, G. I. Zakharkin and S. R. Zhukov, *ibid.* **14** (1978) 1504.
[14] A. M. Khutornoi, G. I. Zakharkin and M. R. Tarasevich, *Zh. Fiz. Khim.* **50** (1976) 255.
[15] B. N. Efremov, G. I. Zakharkin, S. R. Zukov and M. R. Tarasevich, *Elektrokhimiya* **14** (1978) 937.
[16] B. N. Efremov, G. I. Zakharkin, M. R. Tarasevich and S. R. Zhukov, *Zh. Fiz. Khim.* **52** (1978) 1671.
[17] D. M. Shub, A. N. Chemodanov and V. V. Shalaginov, *Elektrokhimiya* **14** (1978) 595.
[18] I. D. Belova, Yu. E. Roginskaya, R. R. Shifrina, S. G. Gagarin, Yu. V. Plekhanov and Yu. N. Venevtsev, *Solid State Comm.* **47** (1983) 577.
[19] N. V. Kozolova, V. V. Shalaginov, V. N. Lomova and D. M. Shub, *Zh. Neorg. Khim.* **28** (1983) 2455.
[20] Ya. M. Kolotyrkin, I. D. Belova, Yu. E. Roginskaya, V. B. Kozhevnikov, D. S. Zakhar'in and Yu. N. Venevtsev, *Mater. Chem. Phys.* **11** (1984) 29.
[21] R. Garavaglia, C. M. Mari and S. Trasatti, *Surf. Technol.* **23** (1984) 41.
[22] C. Pirovano and S. Trasatti, *J. Electroanal. Chem.* **180** (1984) 171.
[23] T. V. Andrushkevich, G. K. Boreskov, V. V. Popovskii, L. M. Plyasova, L. G. Karakchiev and A. A. Ostan'kovich, *Kin. Katal.* **9** (1968) 1244.
[24] I. D. Belova, V. V. Shalaginov, B. Sh. Galyamov, Yu. E. Rosinskaya and D. M. Shub, *Zh. Neorg. Khim.* **23** (1978) 286.
[25] R. Garavaglia, C. M. Mari, S. Trasatti and C. De Asmundis, *Surf. Technol.* **19** (1983) 197.
[26] S. Valeri, G., Battaglin, G. Lodi and S. Trasatti, *Coll. Surf.* **19** (1986) 387.
[27] R. J. Hill, J. R. Craig and G. V. Gibbs, *Phys. Chem. Minerals* **4** (1979) 317.
[28] R. Garavaglia, Thesis, University of Milan (1980).
[29] G. Lodi, G. Zucchini, A. De Battisti, E. Sivieri and S. Trasatti, *Mater. Chem.* **3** (1978) 179.
[30] M. Pourbaix, 'Atlas d'equilibres Electrochimiques', Gauthiers-Villars, Paris (1963).
[31] L. D. Burke, M. E. Lyons and O. J. Murphy, *J. Electroanal. Chem.* **132** (1982) 247.
[32] L. D. Burke and O. J. Murphy, *ibid.* **112** (1980) 379.
[33] R. G. Keil, *J. Electrochem. Soc.* **133** (1986) 1375.
[34] L. D. Burke, M. E. Lyons, E. J. M. O'Sullivan and D. P. Whelan, *J. Electroanal. Chem.* **122** (1981) 403.
[35] S. Ardizzone, A. Carugati and S. Trasatti, *ibid.* **126** (1981) 287.
[36] G. Lodi, A. Daghetti and S. Trasatti, *Mater. Chem. Phys.* **8** (1983) 1.
[37] L. I. Krishtalik, *Electrochim. Acta* **26** (1981) 329.
[38] G. Lodi, E. Sivieri, A. De Battisti and S. Trasatti, *J. Appl. Electrochem.* **8** (1978) 135.
[39] A. Carugati, G. Lodi and S. Trasatti, *J. Electroanal. Chem.* **143** (1983) 419.
[40] S. Trasatti and G. Buzzanca, *ibid.* **29** (1971) App. 1.
[41] G. Battaglin, A. Carnera, G. Della Mea, G. Lodi and S. Trasatti, *J. Chem. Soc. Faraday Trans. 1* **81** (1985) 2995.
[42] B. V. Tilak, C. G. Rader and S. K. Rangarajan, *J. Electrochem. Soc.* **124** (1977) 1879.
[43] J. O'M. Bockris and T. Otagawa, *ibid.* **131** (1984) 290.
[44] S. Trasatti and G. Lodi in 'Electrodes of Conductive Metallic Oxides', Part A (edited by S. Trasatti), Elsevier, Amsterdam (1980) p. 301.